

APPLICATION OF A  
 LOW-FREQUENCY AEROELASTIC ELEMENT METHOD  
 TO THE HARMONIC GUST RESPONSE ANALYSIS  
 OF A FLEXIBLE AIRPLANE

by

H. Ulv Mai  
 Helsinki University of Technology,  
 Otaniemi, Finland

Presented at the XVI OSTIV Congress  
 Chateauroux, France, 1978

ABSTRACT

The low-frequency aeroelastic element method developed recently at Helsinki University of Technology, Finland, is briefly reviewed. In this method, the unsteady aerodynamic forces are calculated by using a low-frequency vortex panel method. The state of motion of the flexible airplane is given in terms of rigid-body modes and measured elastic modes. For comparison, some published experimental and calculated results obtained by this method for the B-47A swept-wing bomber are shown. The method is applied to the harmonic gust response analysis of the PIK-20D sailplane. Calculated plunge, pitch, and wing bending responses in terms of the gust frequency are given. Elastic gust amplification factors and zero-crossing frequencies at four spanwise wing stations are shown in different flight conditions and compared with classical plunge-only values. In some cases, the elastic gust amplification factors are seen to be over 70 per cent in excess of the rigid plunge-only values, which is much more than the common design practice. Possible causes of this are briefly discussed.

SYMBOLS

A	aerodynamic influence matrix
$A_I$	unsteady part of the aerodynamic influence matrix
$A_R$	steady part of the aerodynamic influence matrix
$\bar{A}$	amplification factor
b	span
C	interpolation matrix
D	free-body internal damping matrix
H	transfer function
i	imaginary unit
I	identity matrix
k	reduced frequency
K	free-body stiffness matrix
m	number of modes
M	mass matrix
$N_0$	zero-crossing frequency
O	aeroelastic operator matrix

PRINCIPLES OF  
THE AEPAC METHOD

$P_{kin}$	kinetic pressure
$P$	derivative matrix
$q$	vector of complex mode amplitudes
$s$	number of structural elements
$S$	element area matrix
$T_a$	transformation matrix
$w_g$	vector of complex gust amplitudes
$y$	distance from centerline
$z$	vector of complex element displacement amplitudes
$Z$	mode matrix
$\sigma_w$	intensity of turbulence
$\phi_w$	power-spectral density of gust velocity
$\phi_x$	power-spectral density of load $x$
$\omega$	circular frequency
$\Omega$	matrix of squared mode frequencies

INTRODUCTION

Accurate calculation of loads of a modern, highly flexible sailplane in atmospheric turbulence requires that its complete unsteady aeroelastic behavior is taken into account.

Today, a number of element methods exist for calculating the elastomechanical behavior of a flexible airplane. Very powerful methods exist, too, for the unsteady aerodynamic analysis. Recently at least two large-scale computer codes based on element method techniques have been developed in the United States, combining these tasks to yield a complete aeroelastic analysis system (Ref. 10, 11). However, the existing codes are based on quasi-steady rather than unsteady theories, and they are thus restricted to very low frequencies. Moreover, they require relatively large computer resources, and their usage for small airplane projects (such as sailplanes) is thus hardly justifiable.

To overcome these restrictions, the Laboratory of Light Structures of Helsinki University of Technology launched in 1975 under sponsorship of the Academy of Finland a project for developing an aeroelastic calculation method suitable for the light aircraft projects under way in Finland. The project has now resulted in an aeroelastic computation methodology (Ref. 6) based on the low-frequency vortex panel method (Ref. 5), and materialized in a computer program package called AEPAC (Ref. 7). In the present paper, the AEPAC method is briefly reviewed.

Choosing a low-frequency aerodynamic theory as a basis for an unsteady aeroelastic calculation method is based on the fact that the power-spectral density of atmospheric turbulence decreases very rapidly with increasing frequency. Thus, for harmonic gust response analyses, reasonable calculation errors at high frequencies usually do not seriously worsen the accuracy of load amplification factors and of zero-crossing frequencies, and thus a method of only moderate accuracy at high frequencies but of much reduced cost in comparison with general methods could be useful. The low-frequency vortex panel method (Ref. 5) has been found in practice to be applicable for reduced frequencies up to 0.3 ... 0.4, which is enough for most engineering purposes and is still superior to quasi-steady theories. The AEPAC method has been described in detail in Ref. 6, and we here give only a short summary.

For the element method formulation, the structure is lumped into  $s$  structural mass points having masses  $m_i$  and interconnected with flexible bars. Displacements  $z_i$  of elements are given as sums of elastic deformations with respect to so-called mean axes and rigid-body displacements. For harmonic vibrations the aeroelastic equations of motion for a flexible airplane can be written in the matrix form

$$(1) \quad -P_{kin} T_a S A^{-1} (P + ikC) z + (K + i\omega D - \omega^2 M) z = P_{kin} T_a S A^{-1} w_g$$

(for details, see Ref. 6). This equation can be simplified by approximating the vector  $z$  of complex vibration amplitudes by a complex superposition  $q$  of  $m$  normal modes and rigid-body modes of the system:

$$(2) \quad z \approx Zq$$

In Eq. (2), columns of the modal matrix  $Z$  are nontrivial solutions  $z_n$  of the equation

$$(3) \quad (K - \omega_n^2 M) z_n = 0$$

(Since  $K$  is the free-body stiffness matrix, this set also includes the rigid-body modes). In practice, the elastic modes and frequencies  $\omega_n$  are obtained by a ground-vibration test.

By substituting Eq. (3) into Eq. (1) one obtains

$$(4) \quad [-p_{kin} T_a S A^{-1} (P + ikC) Z + i\omega D Z + MZ(\Omega - \omega^2 I)] q = p_{kin} T_a S A^{-1} w_g$$

Elements of the complex vector  $q$  represent amplitudes of different modes and their relative phase lags.

In the aerodynamic low-frequency theory, the complex aerodynamic influence matrix  $A$  can be written as

$$(5) \quad A = A_R + ikA_I$$

where  $A_R$  and  $A_I$  are real and independent of reduced frequency  $k$ . Moreover, in the low-frequency vortex panel method, elements of  $A_R$  and  $A_I$  are calculable by effective explicit analytic expressions (in more general formulations these elements must be calculated by means of numerical quadratures involving strong singularities). If the aerodynamic influence matrix is given by Eq. (5), then

$$(6) \quad A^{-1} = A_R^{-1} - ikA_R^{-1} A_I A_R^{-1} - \dots$$

The aeroelastic behavior of an aircraft is obtained by solving  $q$  from Eq. (4) for all gust frequencies of interest. Usually  $m$  (the number of modes) is much less than  $s$  (the dimension of  $Z$ ), and then Eq. (4) can be satisfied only in an approximate manner. In Ref. 6, the following method has been adopted for this purpose.

The gust velocity amplitude vector  $w_g$  is approximated by a vector in the subspace  $g$  spanned by column vectors of  $Z$ , and Eq. (4) is premultiplied by  $Z^+$ , the pseudoinverse of  $Z$ . Using Eq. (6) one then arrives at the equation

$$(7) \quad [-p_{kin} (O_{Bo} + ikO_{B1}) + i\omega O_D + O_M(\Omega - \omega^2 I)] q = p_{kin} (O_{Bo} + ikO_{B1}) Z^+ w_g$$

where  $O_{Ao}$ ,  $O_{A1}$  etc. are real  $m$  by  $m$  matrices, which could be called the aeroelastic operator matrices. Their explicit expressions are given in Ref. 6. These matrices are independent of frequency, speed of flight, density of air etc., and they can be calculated once and for all for a given aircraft configuration with a given mass and stiffness distribution. Knowing these matrices, Eq. (7) is relatively easy to solve for  $q$  for every gust frequency,

speed of flight, altitude etc. of interest. The actual state of vibration can then be obtained from Eq. (2), if desired. However, for a load analyst the following interpretation is of much greater importance: If, in connection with the ground vibration test aimed at obtaining the normal mode shapes and frequencies, even strain amplitudes and phase angles are measured for each mode at different locations of the structure, then the superposition  $q$  of these also gives the actual strain state for the flight condition in question. The internal damping is usually neglected in power-spectral calculations.

APPLICATIONS

To test the method, it was applied to a well-known and well-documented test case published in 1961 by Bennett and Pratt (Ref. 1). This report presents an aeroelastic calculation method based on so-called kernel-function techniques together with calculated and flight-test results for the B-47A "Stratojet" bomber. Typical results are shown in Fig. 1, presenting rigid-body plunge and pitch responses, and wing front-spar bending responses. In this figure, the solid line represents flight-test results, the broken line results calculated by Bennett and Pratt (Ref. 1) and the small circles results obtained by the AEPAC method (Ref. 6). The accuracy is seen to be good except between the short-period frequency and the first wing-bending resonance frequency. As explained in Ref. 6, this is probably caused by the fact that a lifting-surface theory (such as the low-frequency

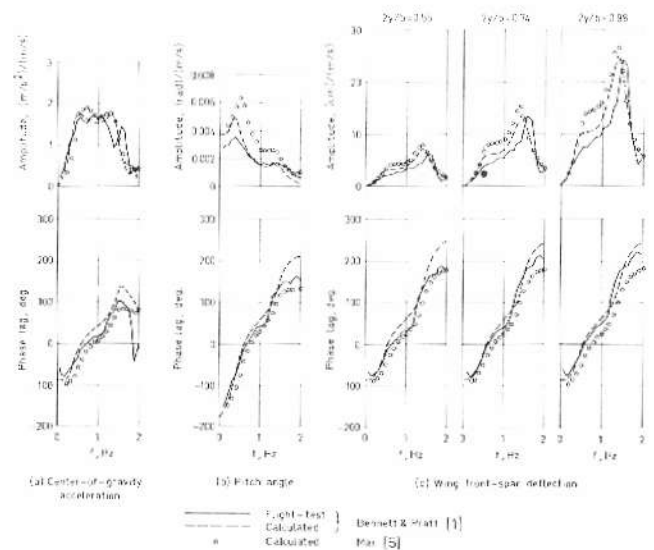


Figure 1. Harmonic gust response of the B-47A bomber.

vortex panel method) is unable to account for fuselage and nacelle effects on the maneuver point location. This in turn causes a slightly too large short-period frequency, and consequently a too strong interference between the pitch responses and the wing-bending resonance. However, if this diagnosis is correct, then the error in response calculations caused by an erroneous maneuver point is always conservative from a load analyst's point of view.

We now turn our attention to applications of the AEPAC method to the PIK-20D sailplane. These calculations aimed at obtaining a realistic fatigue spectrum due to atmospheric turbulence. They are discussed in detail in Refs. 8 and 9. To describe the behavior of the airplane in question, the six modes given in Table 1 were used. Shapes and frequencies of elastic modes were determined by a ground vibration test (Ref. 4). It is worth noting that inclusion of the second symmetric wing bending mode proved to be an important choice. This is because through the whole frequency range of interest the second wing bending mode was almost opposite in phase to the first wing bending mode. This had the result that the bending strain distribution was much nearer the static load distribution (and probably more realistic) than it had been, if only the first wing bending mode had been considered. Some calculated results are shown in Fig. 2. Unfortunately, at the moment, flight-test results

Table 1 PIK-20D modes

Mode No.	Mode	Frequency Hz
1	Rigid-body vertical translation (plunge)	0
2	Rigid-body angular displacement (pitch)	0
3	First symmetric wing bending mode	2.94
4	Second symmetric wing bending mode	8.85
5	First symmetric wing twist mode	27.60
6	First fuselage bending mode	9.80

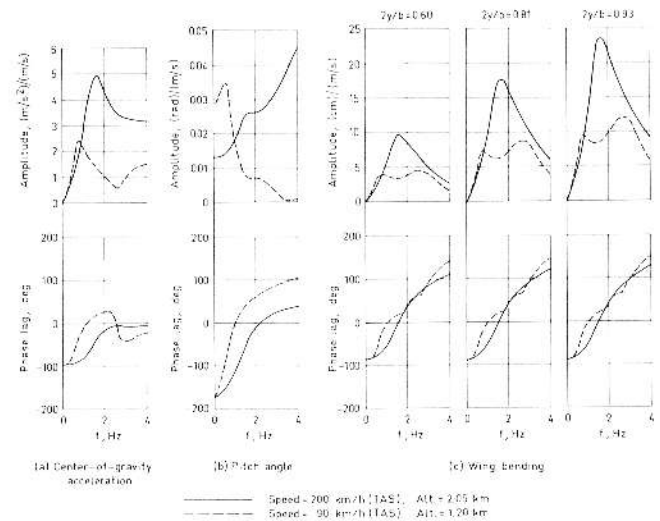


Figure 2. Harmonic gust response of the PIK-20D sailplane.

concerning the aeroelastic behavior of the PIK-20 have not yet been analyzed, so that a comparison between calculated and flight-test results similar to that given previously for the bomber is not available.

There are two important coefficients of interest in construction the fatigue test spectrum, viz., the amplification factor

$$(8) \quad \bar{A} = \frac{1}{\sigma_w} \left[ \int_0^\infty \phi_x(\omega) d\omega \right]^{1/2} = \frac{\sigma_x}{\sigma_w}$$

and the zero-crossing frequency

$$(9) \quad N_0 = \frac{1}{2\pi\sigma_x} \left[ \int_0^\infty \omega^2 \phi_x(\omega) d\omega \right]^{1/2}$$

In Equations (8) and (9),

$$(10) \quad \sigma_w = \left[ \int_0^\infty \phi_w(\omega) d\omega \right]^{1/2}$$

is the intensity of the turbulence.  $\phi_x$  and  $\phi_w$  represent power-spectral densities of the load  $x$  in question and gust velocity, respectively.

The power-spectral density of the load is obtained from the well-known equation

$$(11) \quad \phi_x(\omega) = |H(i\omega)|^2 \phi_w(\omega)$$

For PIK-20D calculations, the von Kármán spectrum was used for  $\phi_w$ . The modulus of the transfer function  $H$  is represented by a curve similar to those presented in Figs. 1 and 2, drawn for the load of interest.

It is a common practice first to calculate the amplification factor  $\bar{A}$  and the zero-crossing frequency  $N_0$  for a nonpitching point-like rigid airplane, and then to multiply the results by

experimentally determined factors taking into account effects of elasticity, fuselage etc. The rigid response is obtained from simple charts. Elasticity corrections for the amplification factor vary from case to case, but factors ranging from 1.15 to 1.25 seem to be typical for transport airplanes (Ref. 3, 12). However, values as high as 1.6 have been proposed (Ref. 2). A comparison between rigid-body, corrected rigid-body, and actual aeroelastic amplification factors is shown in Fig. 3 for PIK-20D in two different flight conditions. This figure also contains a similar comparison for the zero-crossing frequency. In this figure, the elasticity correction factor 2 was used for  $N_0$ .

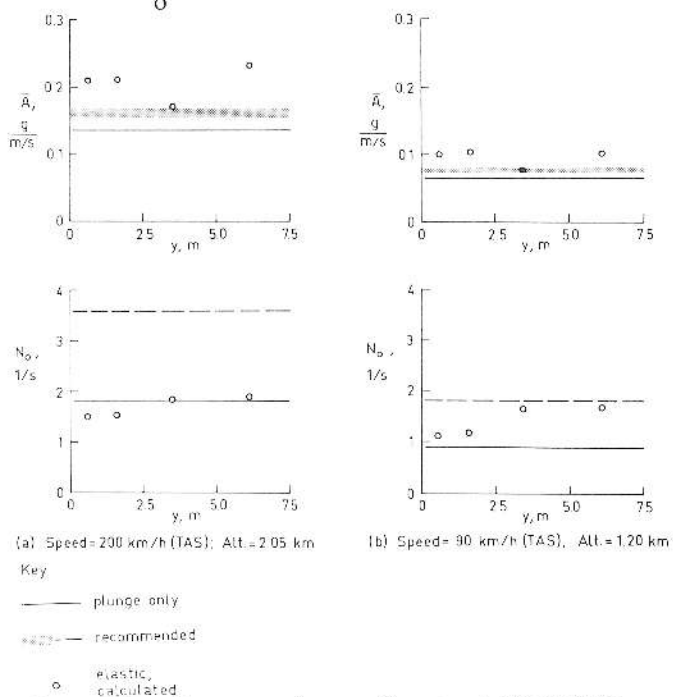


Figure 3. A comparison of g-amplification factors  $\bar{A}$  and zero-crossing frequencies  $N_0$  of the PIK-20D sailplane.

The comparison reveals two interesting features. First, the amplification factors are not the same for all wing stations. For instance in the PIK-20D wing case the root and the tip are more susceptible to fatigue than other portions of the wing. Second, amplification factors are seen in almost all cases to be in excess of the common design practice; the largest value is about 1.72. This may be partially caused by the load over-estimation between the short-period frequency and the wing-bending resonance frequency discussed above. However, we feel that this does not suffice to explain the whole amplification factor excess. It is possible that for highly flexible reinforced plastic airplanes the common design recommendations for the

elasticity correction factor should be revised. Anyway, we think that this problem is worth a serious consideration. The flight test program currently under way at the Laboratory of Light Structures of Helsinki University of Technology may cast more light upon this problem.

REFERENCES

1. Bennett, F. V. and Pratt, K. G., "Calculated Responses of a Large Sweptwing Airplane to Continuous Turbulence with Flight-Test Comparisons." Washington, D.C., 1961. NASA Technical Report R-69.
2. Buxbaum, O. und Gassner, E., "Häufigkeitsverteilungen als Bestandteil der Lastannahmen für Verkehrsflugzeuge." Darmstadt, 1966. Lab. für Betriebsfestigkeit, Bericht Nr. FB-68.
3. Firebaugh, J. M., "Evaluations of a Spectral Gust Model Using VHG and V-G Flight Data," *J. Aircraft*, 4(1967)6, pp. 518-525.
4. Kokko, J., "PIK-20B siiven värähtelymittauset." Otaniemi, 1976. Helsinki University of Technology, Lab. of Light Structures (unpublished report).
5. Mai, H. U., "A Vortex Panel Method for Slowly Oscillating Lifting Surfaces at Subsonic Speeds." Otaniemi, 1976. Helsinki University of Technology, Lab. of Aerodynamics, Report No. 76-A1.
6. Mai, H. U., "A Low-Frequency Aeroelastic Element Method and Its Application to the Harmonic Gust Response Analysis of a Flexible Airplane." Helsinki, 1978. *Acta Polytechnica Scandinavica*, No. Me 74.
7. Mai, H. U., "AEPAC - The Aeroelastic Program Package." Otaniemi, 1978. Helsinki University of Technology, Lab. of Light Structures, Report.
8. Nyström, S., "Statiskt och dynamiskt hållfasthetsprov för en segelflygplansvinge." Jämijärvi, 1977. M. Sc. Thesis, Helsinki University of Technology, Department of Mechanical Engineering.
9. Nyström, S. and Mai, H. U., "A Fatigue Test on a Sailplane Wing." Paper presented at XVth OSTIV Congress at Châteauroux (France), July 20 to 29, 1978.

(Continued on page 42)